

Article

Simulation and Experimental Evaluation of a Refractive-Reflective Static Solar Concentrator

Guillermo Luque-Zuñiga ¹, Rubén Vázquez-Medina ¹, G. Ramos-López ^{1,*},
David Alejandro Pérez-Márquez ² and H. Yee-Madeira ^{3,*}

¹ Instituto Politécnico Nacional, CICATA Unidad Querétaro, Querétaro 76090, Mexico

² Departamento de Ingeniería en Diseño Industrial, Universidad Politécnica del Bicentenario, Guanajuato 36283, Mexico

³ Instituto Politécnico Nacional, Escuela Superior de Física y Matemáticas, Unidad Profesional Adolfo López Mateos Zacatenco, Ciudad de Mexico 07320, Mexico

* Correspondence: gramos@ipn.mx (G.R.-L.); hernaniyee@hotmail.com (H.Y.-M.);
Tel.: +52-442-1587466 (G.R.-L.)

Abstract: Static solar devices have advantages over solar tracking systems. In pure reflective systems, solar reception is limited by the entry angle of the reflector. Many reflective systems are based on mirror Compound Parabolic Concentrators. The solar collection can be improved by placing a lens on top of the reflector. In this work, a static system is proposed, consisting of a mirror funnel concentrator with a prism on top. The system is designed using ray-tracing software and is subsequently built and experimentally evaluated. The system designed for an effective concentration factor of $4\times$ reaches an effective concentration of $3.2\times$ at 11:30 a.m. and has an acceptance angle of 60° . Considering the time interval from 8 a.m. to 4 p.m., the system harvests 30.7% more energy than the flat surface. If the time interval considered is from 9:30 a.m. to 2:30 p.m., the increase in harvest is $\sim 77\%$. The incorporation of the prism represents an increase of $\sim 6\%$ compared to the bare reflective system.

Keywords: solar concentrator; refractive-reflective system; collected energy; solar energy



Citation: Luque-Zuñiga, G.; Vázquez-Medina, R.; Ramos-López, G.; Pérez-Márquez, D.A.; Yee-Madeira, H. Simulation and Experimental Evaluation of a Refractive-Reflective Static Solar Concentrator. *Energies* **2023**, *16*, 1071. <https://doi.org/10.3390/en16031071>

Academic Editor: Manolis Souliotis

Received: 19 December 2022

Revised: 6 January 2023

Accepted: 13 January 2023

Published: 18 January 2023



Copyright: © 2023 by the authors. Licensee MDPI, Basel, Switzerland. This article is an open access article distributed under the terms and conditions of the Creative Commons Attribution (CC BY) license (<https://creativecommons.org/licenses/by/4.0/>).

1. Introduction

Solar static systems are cheaper than solar tracker systems. Even designing solar collection devices with larger acceptance angles for less accurate solar trackers is seen as a cost reduction [1]. Static concentration systems, having a low concentration ratio, can be used with common commercial silicon cells, so-called “one sun” cells [2,3]. Coello et al. observed an increase in PV generation with common solar cells up to a concentration ratio of $15\times$. Another study, choosing PV cells randomly in the market, shows that in some cases this benefit is limited to $3\times$ [4]. The combination of static concentrators and common PV cells can reduce costs in photovoltaic applications.

Many of the solar concentrators presented in the literature use mirrors or reflecting surfaces [5–13]. Others make use of total internal reflection in the walls of solid dielectric materials, or a combination of both [1,6,9]. Many of the systems use Compound Parabolic Concentrators (CPC), either as mirrors or as solid dielectric concentrators. CPCs only collect energy at angles of incidence smaller than the half acceptance angle [11]. In a recent study, it was observed that other geometries, like the funnel, can have a better energy collection [14]. There is another group of systems, that combine a lens (or prism) on top of the reflective concentrating device [1,10,12,13,15]. The use of combined systems allows the improvement of certain aspects, such as increasing the optical efficiency, increasing the time of collection of solar energy and maintaining the temperature above certain values. Su et al. remarks on the importance of reducing the amount of dielectric material in the concentrating devices [6].

A direct comparison between systems is difficult since there are linear [1,12] and axial systems [6,9,13,15]. Some systems include only numerical simulations [1], whereas other systems include also experimental evaluations of certain aspects [5–7,9,12,13,15].

In this work, the design, construction and experimental evaluation of a funnel refractive static solar concentration system with a prismatic lens on top is carried out. The investigation is divided into 3 sections, in the first, the concentration system is presented, in the second the details of both theoretical and experimental evaluation are described and finally the comparison of results is done.

2. System Details

The concentration system is composed of a reflective Funnel and a prismatic refractive lens on top of it, as shown schematically in the cross-section of Figure 1. Only the inner wall of the Funnel is reflective with a reflectivity of 96%, and a concentration factor of $4\times$. This concentration factor is the Geometrical Concentration Ratio (GCR) calculated using Equation (1). The receptor is placed at the bottom of the Funnel.

The funnel has a height of 75 mm, an inlet diameter of 75 mm and an outlet diameter of 37.5 mm. So, the inlet opening area is 4417.86 mm^2 while the outlet opening is 1104.47 mm^2 .

The prism is a single piece of dielectric material (Polymethylmethacrylate PMMA). The base is a cylinder 5 mm high and the top is a cone with an angle of 12° . The outer diameter is 75 mm (see Figure 1). The dielectric material has a nominal refractive index of $n = 1.49$ [16].

$$\text{GCR} = \frac{\text{aperture area}}{\text{receiver area}} \quad (1)$$

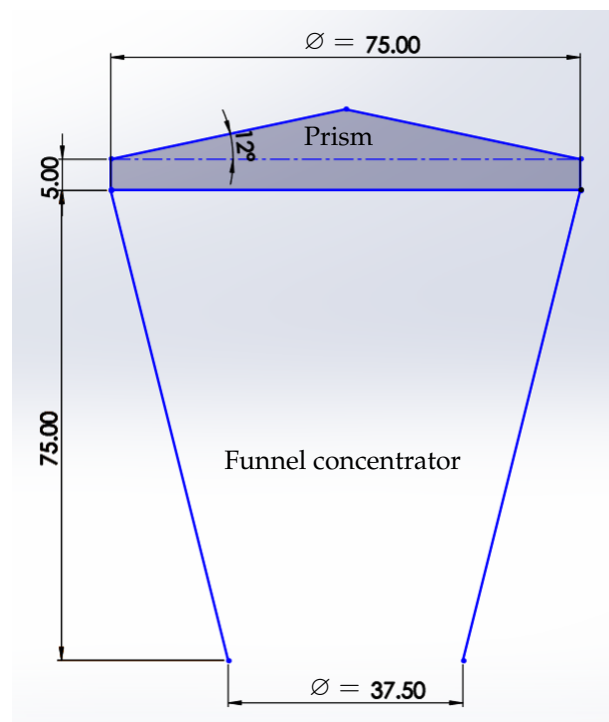


Figure 1. Cross section of the concentration system composed by the reflective Funnel and the refractive Prism (Dimensions in mm).

3. Evaluation Details

3.1. Ray-Tracing Evaluations

For the ray-tracing evaluation, OptiCAD [17] was used. For the sun, an irradiance of 1000 W/m^2 was considered for normal incidence (zenith). The simulations were carried out under the following considerations: The system is placed in the Equator, with the receptor

horizontally, in the Equinox; the sun varies its apparent position from 8:00 a.m. to 4:00 p.m.; the simulations are made at 30 min intervals; the sun rays have a divergence of 0.53° and all have the same energy.

The prism is simulated with a refractive material with a refractive index of 1.49, but without surface reflectivity. The receiver is a circular absorbing plate with 0% reflectivity and 100% absorbance, placed 3 mm below the system, as shown in Figure 2. This position of the absorber was chosen to adequately represent the experimental conditions that are used in the laboratory prototype for evaluation.

Figure 2 shows the typical path of rays falling on the system for an angle of incidence of 22.5° . In the absence of the prism, the rays that enter through the upper opening can reach the receiver either directly (ray R1), or after one or several reflections (rays R2 and R3). They can also be reflected out of the system, as is the case of ray R4. Ray R4 undergoes several reflections but finally leaves the system through the upper opening (Figure 2a). In the presence of the prism, the trajectory of the rays is more complex. In Figure 2b the rays that fall on the central part of the prism will suffer a slight deviation and most of them will reach the receiver either directly (ray R1') or after one or more reflections (rays R2', R3' and R4'). The R4' ray corresponds to the R4 ray of Figure 2a, which was reflected out of the system. As can be seen, at this angle of incidence, the prism helps rays such as R4' reach the receiver, thus increasing the solar harvest.

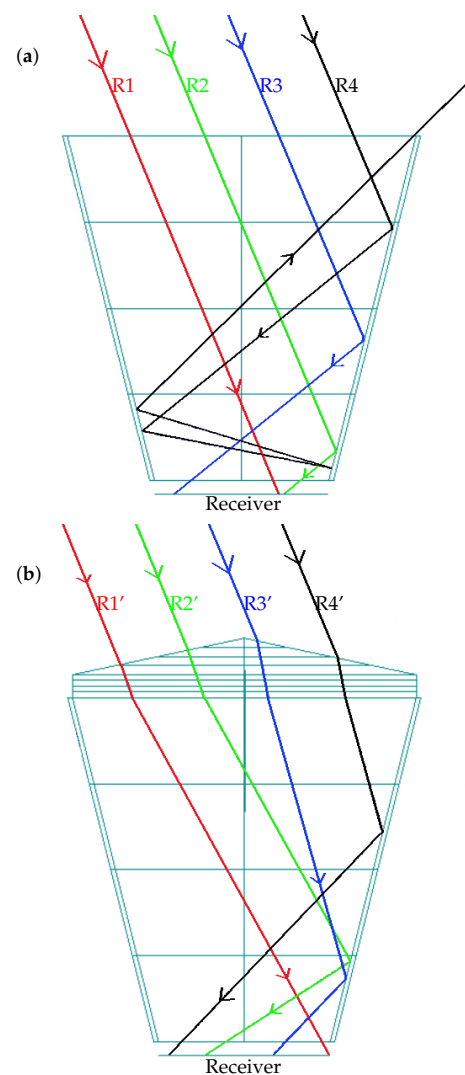


Figure 2. Path of typical rays falling on the system: (a) bare funnel concentrator, (b) refractive-reflective system, with an incidence angle of $\theta = 22.5^\circ$.

The beneficial effect of the prism is only for angles of incidence smaller than $\pm 37.5^\circ$. For larger angles, the majority of the rays undergo multiple reflections and leave the concentrator.

Figure 3 shows the results of the simulations made for the funnel concentrator with prism (Funnel-Prism SIM) and without prism (Funnel SIM), respectively. The collected energy is the total energy flux that strikes the receiver at a given time of day, in units of W/m^2 . For the bare funnel, the solar harvest before 9:00 a.m. is negligible. At 9:30 a.m., $217.45 \text{ W}/\text{m}^2$ are harvested in the receiver. Later the harvest increases, until it reaches a maximum of $3203.65 \text{ W}/\text{m}^2$ at solar noon, to decrease afterwards. The addition of the prism to the funnel has very similar behaviour, however, there is a solar harvest already at 8:30 a.m. ($11.08 \text{ W}/\text{m}^2$). While the harvest without the prism is higher in the interval between 9:05 a.m. and 10:15 a.m., the prism allows a better solar harvest between 10:15 a.m. and 11:30 a.m. The effect is more visible at 10:30 a.m. when the prism allows a 23% higher harvest. However, at solar noon the prism produces a slight decrease in the harvest, of less than 2%. In this way the total improvement of the addition of the prism is approximately 1% compared to the bare funnel, giving a total harvest 54% larger than for a flat plate.

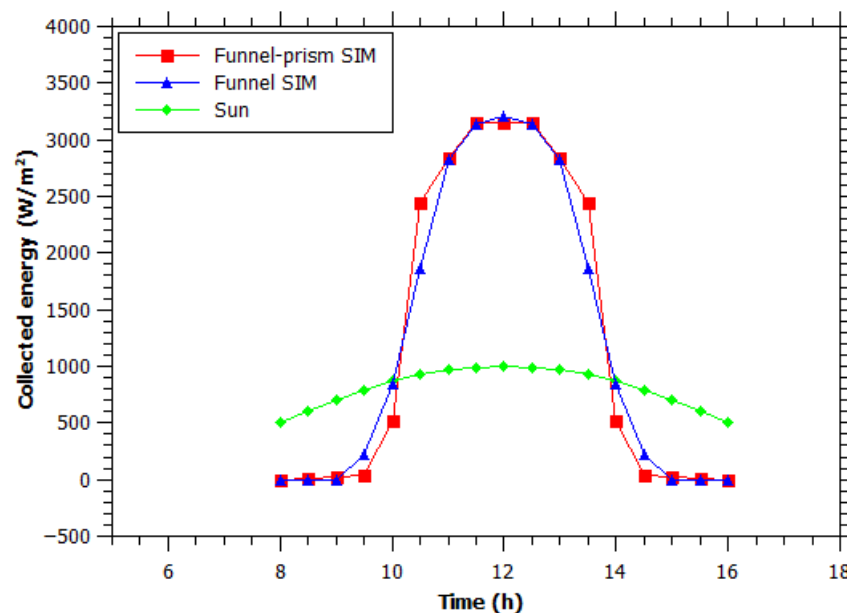


Figure 3. Collected energy as obtained with ray-tracing simulations.

3.2. Experimental Evaluation

While optical ray-tracing evaluations are very reliable, they consider idealized surfaces and optical properties. Sometimes these idealized conditions are difficult or very expensive to reproduce in the lab or in the prototypes. The experimental evaluation of a prototype developed without highly sophisticated tools can give us an idea of what, in general, can be expected from the design.

The Funnel was manufactured with a reflective aluminium sheet of about 1 mm thickness. A truncated cone-shaped wooden core was manufactured with the appropriate diameters (75 mm and 37.5 mm, respectively). On this core, the aluminium sheet was moulded. To keep the shape it was wound with wire and finally glued with epoxy glue. Figure 4a shows an upper image of the funnel and the concentration pattern at normal incidence. The manufactured shape is not perfect, particularly in the position of the joints of the sheets.



Figure 4. (a) Upper view of the funnel and concentration pattern, (b) Image of the prism and concentration pattern.

The prism was cut from a 3" diameter PMMA cylinder. Subsequently, it was polished using different grades of silicon carbide sandpaper, until a surface of sufficient optical quality was obtained. The final polish was done with car headlight repair fluid. Figure 4b shows the polished prism and the typical concentration pattern in the sun.

A lateral image of the system is shown in Figure 5. To minimize the deformation that could be caused by the clamping of the system, a cylindrical support was developed, on which the system was seated for evaluation (black in Figure 5).

For the measurements, a 100 W tungsten halogen lamp powered by a regulated voltage supply of radiometric quality was used as the light source. The lamp bulb was placed at the distance at which the dimensions of the filament produced a divergence of 0.53° . This was done to emulate the ray divergence of the solar disk. To do the measurements for the different hours of the day, the light source was placed at the corresponding height and distance, as shown in Figure 6. The marks corresponding to each measurement can be seen in the table.

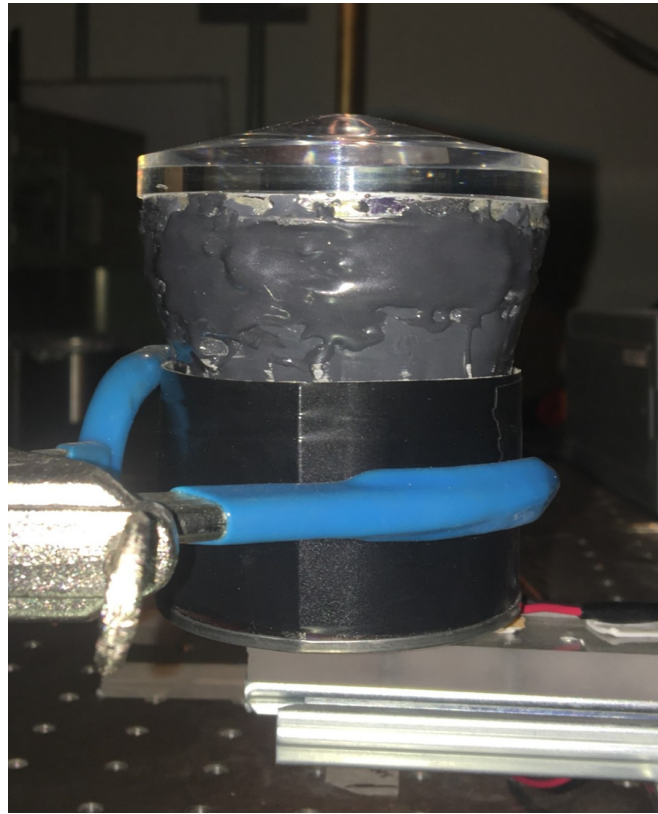


Figure 5. Lateral view of the system ready to be measured.

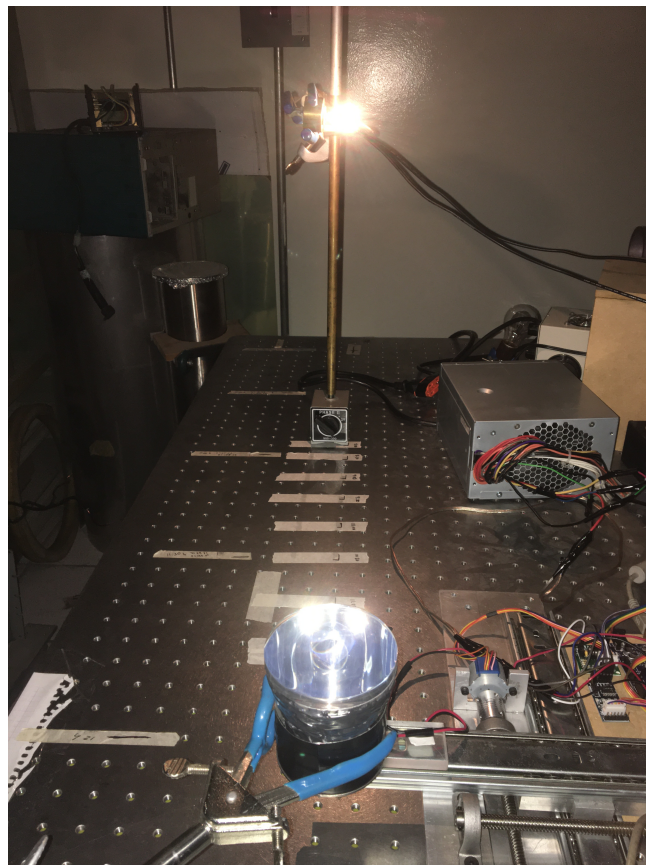


Figure 6. Experimental setup showing the lamp, the marks on the table, the system and XY positioning system together with the electronics.

An XY displacement system was developed to obtain the intensity measurements and the concentration patterns. The signal of the silicon photodiode is amplified using an operational amplifier, and the position is controlled by stepper motors. A microcontroller moves the diode to the desired position and stores the data in a non-volatile memory. The XY displacement system is programmed to obtain the measurements in a matrix of 20×20 bins, which covers the entire area of the receiver.

First, the measurements in the absence of the concentration system were made, adjusting the intensity of the light source so that it gave the equivalent of 1000 W/m^2 at solar noon. Moving the light source to the different positions corresponding to the different hours of the day, the data of the “Sun” curve of Figure 7 was obtained. Although it cannot be seen very well in the graph, the data agree good with the cosine curve.

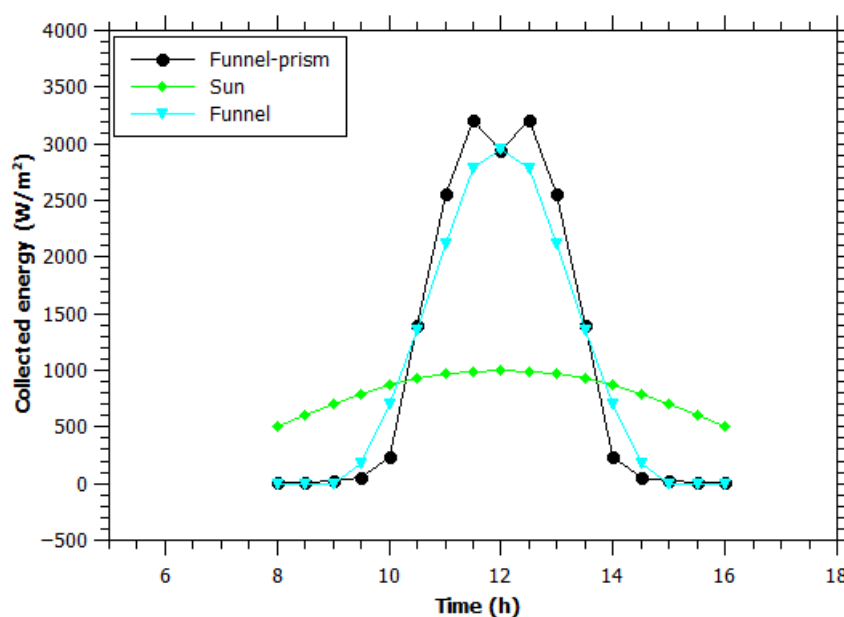


Figure 7. Experimental data of the collected energy.

Next, the curves with the bare funnel (Funnel curve in Figure 7) and the complete system (Funnel-Prism curve in Figure 7) were measured. For the Funnel curve (cyan curve), the energy harvest before 9:00 a.m. is negligible. Energy harvest starts at 9:30 a.m. (180 W/m^2), and increases rapidly between 9:30 and 11:30 a.m. Harvest reaches a maximum of 2953.27 W/m^2 at solar noon. The Funnel-prism curve (black curve), although hardly seen in Figure 7, does not start at zero. Already at 8:00 a.m. 11.97 W/m^2 are harvested. As in the previous case, the harvest increases rapidly between 9:30 and 11:30 a.m., reaching a maximum of 3203.36 W/m^2 at 11:30 a.m. For this time of the day, the angle of incidence is 7.5° and the harvest factor is 3.2 times the harvest without the device. In contrast to the bare funnel, the energy harvest is slightly less at solar noon (2940.15 W/m^2). This implies a decrease of 8%, which contrasts with the value of less than 2% from the simulations.

As can be seen, the addition of the prism has the most noticeable effect increasing the solar harvest between 10:30 a.m. and 1:30 p.m. The solar harvest between 8 a.m. and 4 p.m. without the system is 6.85 kW/m^2 . The harvest in the same period with the bare funnel concentrator is 8.6 kW/m^2 . This implies a 25.47% increase in harvest. The complete system has a harvest of 8.96 kW/m^2 in the same period (30.7% larger than without the system). If the time interval considered is only from 9:30 a.m. to 2:30 p.m., the improvement in the harvest is 76.78%.

4. Results

Figure 8 shows the comparison between the measurements and the simulations for the complete system. The general trend of the two curves is similar. However, the experimental curve is narrower than the simulation and the depression at solar noon is larger in the measurement than in the simulation. Another difference is that the harvest at 10:30 a.m. in the measurement is approximately 60% of the expected value according to the simulations. This difference is attributable to manufacturing inaccuracies, mainly in the funnel.

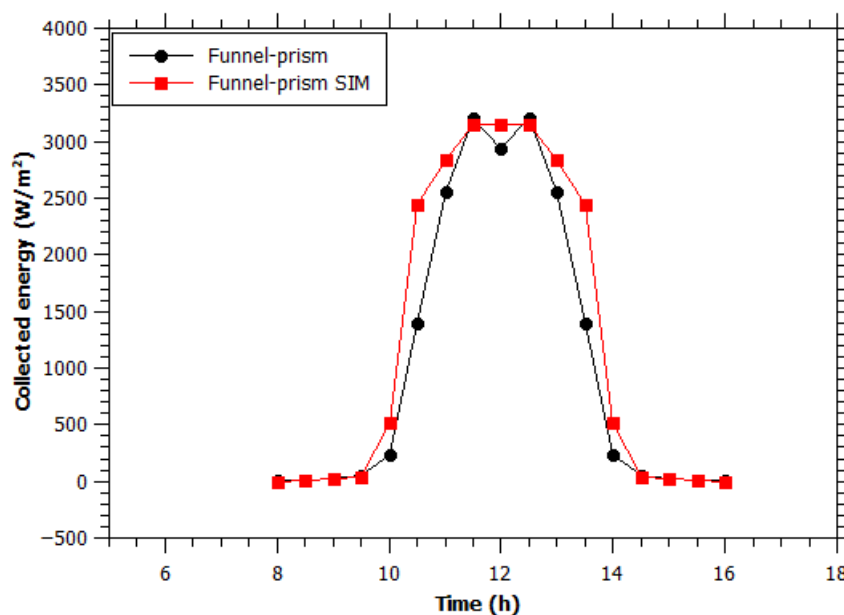


Figure 8. Comparison of experimental(Funnel-prism) and simulated data (Funnel-prism SIM) for the complete system.

In compound parabolic concentrators (CPCs) the acceptance angle and the concentration ratio are linked. Su et al. [6] obtained a concentration ratio of $4\times$ with an acceptance angle of 29° . To have an acceptance angle comparative to ours of 47° they had to reduce the concentration ratio to $2.5\times$. In our system, using the Funnel, a geometric concentration ratio of $4\times$ can be achieved with an acceptance angle of about 52° . Baig et al. [9] using a refractive tridimensional solid dielectric CPC together with a reflective casing designed the system for a concentration ratio of $3.6\times$. This system obtained under the best experimental conditions a power factor of 2.76. In contrast, our system reaches an experimental concentration factor of $3.2\times$ using much less dielectric material.

As mentioned before, the comparison with linear systems is difficult. Vu et al. [1] designed a linear system with some elements similar to ours: a concentrating CPC with a prism on top of it. The system is intended to reduce costs using less accurate solar trackers instead of highly accurate ones. Different to ours, the CPC is a solid dielectric and concentrates due to total internal reflection. The system is designed for a high concentration ratio of $50\times$ with an acceptance angle of 6° , thus making a direct comparison almost impossible. Li et al. presented a linear concentrator with a curved PMMA Fresnel lens on top [18] intended for air heating. The linear concentrator was an aluminium V-channel with 0.92 reflectivity. A concentration factor of $2.5\times$ was achieved, but with an acceptance angle of only 19° . Our system has a higher concentration factor with more than twice the acceptance angle. It also has the advantage of being a simple system, since it uses a prism instead of a complicated curved Fresnel lens.

Coello et al. [3] describes only small variations of efficiency of a one-sun solar cell when used with concentrations less than $15\times$. A solar cell with an efficiency of 14% at one

sun shows the efficiency of 15% at $3\times$. Taking this into account if used for photovoltaic applications the electrical harvest at the best performance of our system would imply more than three times the electrical production of the bare cell. Integrated over the whole day, the benefit would be about 1.6 times the energy production of the bare cell, as our system only collects sunlight for a little more than 4 h. All these considerations hold only if the solar cell is kept at 25° and the illumination pattern is reasonably homogeneous, a topic that requires further evaluation.

Figure 9 shows the optical efficiency of the system measured experimentally, at different times. For this evaluation, the light intensity at the entrance of the system and the integral measurement of light at the receiver was measured. The maximum optical efficiency is reached at 11:30 with a value of 69.36%. This value is slightly lower than that reported by other authors for static concentration systems (Baig et al. [9]).

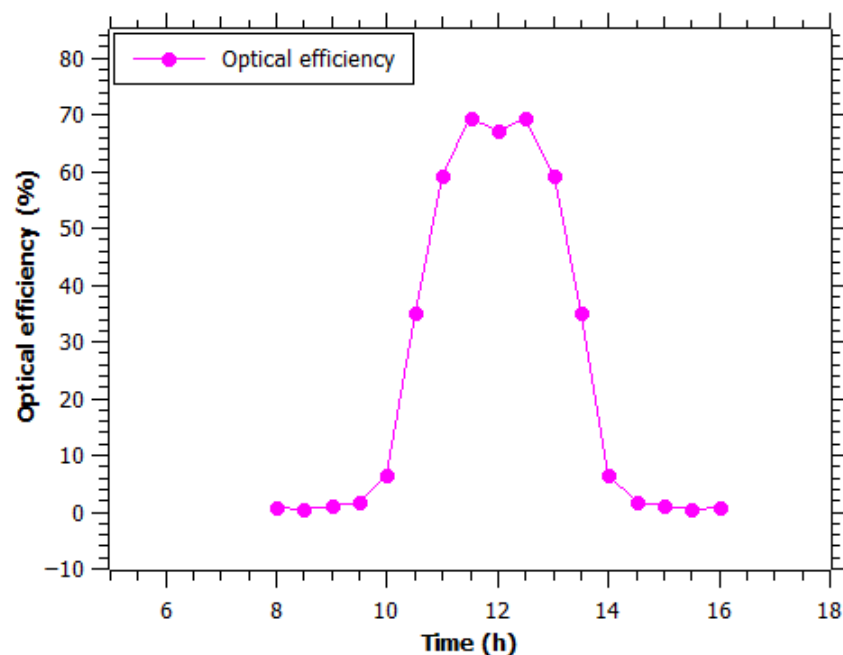


Figure 9. Experimental optical efficiency.

5. Conclusions

This work describes a double static concentrator, based on a refractive prism on top of a funnel with internally reflective walls. The geometry of the pieces is relatively simple and easy to manufacture. The best performance is achieved for acceptance angles between -22.5° and $+22.5^\circ$, for which the concentration factor is larger than $1\times$. An effective concentration factor of $3.2\times$ is reached at 11:30 h.

With the incorporation of the prism, the solar harvest of the funnel increases. The funnel has an acceptance angle of $\sim 52.5^\circ$, and with the addition of the prism, it increases to $\sim 60^\circ$. The double system has a maximum experimental optical efficiency of 69.36%, which could be increased by improving the manufacturing quality of the prism and the funnel.

Considering the time interval from 8 a.m. to 4 p.m., the system harvests 30.7% more energy than the flat surface. If the time interval considered is from 9:30 a.m. to 2:30 p.m., the increase in harvest is $\sim 77\%$. The incorporation of the prism represents an increase of $\sim 6\%$ compared to the bare reflective system.

As the receiver geometry is flat, the concentration system can be used for photovoltaic or photo-thermal applications. Besides its simplicity, the system has the additional benefit of using a little amount of refractive material.

Author Contributions: Conceptualization, G.L.-Z. and G.R.-L.; methodology, G.L.-Z., G.R.-L. and H.Y.-M.; validation, R.V.-M. and D.A.P.-M.; investigation, G.L.-Z., G.R.-L.; resources, G.R.-L.; data curation, H.Y.-M. and D.A.P.-M.; writing—original draft preparation, G.L.-Z.; writing—review and editing, G.R.-L., H.Y.-M., R.V.-M. and D.A.P.-M.; All authors have read and agreed to the published version of the manuscript.

Funding: This research was funded by Instituto Politécnico Nacional, México, with grant SIP20220933.

Data Availability Statement: All data supporting the experiments and the conclusions of the study are included within the article, and additional data can be obtained from the corresponding author upon request.

Conflicts of Interest: The authors declare no conflict of interest.

References

1. Vu, N.H.; Shin, S. A Concentrator Photovoltaic System Based on a Combination of Prism-Compound Parabolic Concentrators. *Energies* **2016**, *9*, 645. [CrossRef]
2. Amanlou, Y.; Tavakoli, H.T.; Ghobadian, B.; Najafi, G.; Mamat, R. A comprehensive review of Uniform Solar Illumination at Low Concentration Photovoltaic (LCPV) Systems. *Renew. Sustain. Energy Rev.* **2016**, *60*, 1430–1441. [CrossRef]
3. Coello, J.; Castro, M.; Anton, I.; Sala, G.; Vazquez, M.A. Conversion of Commercial Si Solar Cells to Keep Their Efficient Performance at 15 Suns. *Prog. Photovoltaics Res. Appl.* **2004**, *12*, 323–331. [CrossRef]
4. Pérez-Márquez, D.A. Sistema de Concentración Solar Semiestático para Celdas Fotovoltaicas. Ph.D. Thesis, Instituto Politecnico Nacional, Ciudad de Mexico, Mexico, 2015. (In Spanish)
5. Kaiyan, H.; Hongfei, Z.; Tao, T.; Xiaodi, X. Experimental investigation of high temperature congregating energy solar stove with sun light funnel. *Energy Convers. Manag.* **2009**, *50*, 3051–3055. [CrossRef]
6. Su, Y.; Pei, G.; Riffat, S.B.; Huang, H. A Novel Lens-Walled Compound Parabolic Concentrator for Photovoltaic Applications. *ASME J. Sol. Energy Eng.* **2012**, *134*, 021010. [CrossRef]
7. Zheng, H.; Wu, G.; Tao, T.; Su, Y.; Dai, J. Combination of a light funnel concentrator with a deflector for orientated sunlight transmission. *Energy Convers. Manag.* **2014**, *88*, 785–793. [CrossRef]
8. Shanks, K.; Baig, H.; Senthilarasu, S.; Reddy, K.S.; Mallick, T.K. Conjugate refractive–reflective homogeniser in a 500× Cassegrain concentrator: Design and limits. *IET Renew. Power Gener.* **2016**, *10*, 440–447. [CrossRef]
9. Baig, H.; Chemisana, D.; Sundaram, S.; Mallick, T. Conjugate refractive–reflective based building integrated photovoltaic system. *Mater. Lett.* **2018**, *228*, 25–28. [CrossRef]
10. Gupta, M.; Kumar, D.A.; Kumar, V.; Singh, M.D. Solar concentrator based multipurpose sunlight harvesting system without tracking. *OSA Continuum.* **2019**, *2*, 667. [CrossRef]
11. Guiqiang, L. Design and Development of a Lens-walled Compound Parabolic Concentrator—A Review. *J. Therm. Sci.* **2019**, *28*, 17–29.
12. Jin, R.; Zheng, H.; Ma, X.; Zhao, Y. Performance investigation of integrated concentrating solar air heater with curved Fresnel lens as the cover. *Energy* **2020**, *194*, 116808. [CrossRef]
13. Kumar K.B.; Gupta, M.; Singh, M.D. Efficient sunlight harvesting with combined system of large Fresnel lens segmented mirror reflectors and compound parabolic concentrator without tracking sun for indoor daylight illumination. *Renew. Energy* **2023**, *202*, 1198–1214. [CrossRef]
14. Luque-Zuniga, G.; Ramos, G.; Yee-Madeira, H.T.; Perez-Marquez, D.A.; Vázquez-Medina, R. Numerical investigation of three solar static concentrators with the same geometrical concentration rate. *Energy Sci. Technol. Manag.* **2021**, *1*, 16–20.
15. Wang, D.; Lan, T. Design of a gradient-index lens with a compound parabolic concentrator shape as a visible light communication receiving antenna. *Appl. Opt.* **2018**, *57*, 1510–1517. [PubMed]
16. Baker, A.K.; Dyer, P.E. Refractive-Index Modification of PolyMethylMethAcrylate (PMMA) Thin Films by KrF-Laser Irradiation. *Appl. Phys.* **1993**, *A57*, 543–544. [CrossRef]
17. Optical Analysis Program OptiCAD™, Opticad Corporation, 511 Juniper Drive, Santa Fe (NM), 87501 USA. Available online: https://www.phenix.bnl.gov/phenix/WWW/publish/barish/publish/wasiko/Copy/Solar/OP_MANUAL.pdf (accessed on 7 December 2022).
18. Li, G.; Pei, G.; Su, Y.; Wang, Y.; Yu, X.; Ji, J.; Zheng, H. Improving angular acceptance of stationary low-concentration photovoltaic compound parabolic concentrators using acrylic lens-walled structure. *J. Renew. Sustain. Energy* **2014**, *6*, 013122. [CrossRef]

Disclaimer/Publisher’s Note: The statements, opinions and data contained in all publications are solely those of the individual author(s) and contributor(s) and not of MDPI and/or the editor(s). MDPI and/or the editor(s) disclaim responsibility for any injury to people or property resulting from any ideas, methods, instructions or products referred to in the content.